

## Supporting Information

### **Highly selective defect-mediated photochemical CO<sub>2</sub> conversion over fluorite ceria at ambient conditions**

*Dong Jiang, Wenzhong Wang,\* Erping Gao, Songmei Sun, and Ling Zhang*

## ***Experimental details, ESI.***

**Chemicals and characterization.** All the reagents were of analytical purity and used as received without further purification. NaOH and NaBH<sub>4</sub> is purchased from Sinopharm Reagent Co. Ltd. Ce(NO<sub>3</sub>)<sub>3</sub>·6H<sub>2</sub>O is obtained from Aladdin reagents, Shanghai. X-ray diffraction (XRD) patterns were recorded on a Rigaku D/MAX 2250V diffractometer using monochromatized Cu K $\alpha$  ( $\lambda=0.15418$  nm) radiation. The Si powder (99.999%) obtained from Alfa Aesar is used as the inner standard (mixed with 10 wt %). Transmission electron microscopy (TEM) images were performed on a JEOL JEM-2100F, with an accelerating voltage of 200 kV. UV-vis diffuse reflectance spectra (DRS) of the samples were obtained on a UV-vis spectrophotometer (Hitachi U-3010) using BaSO<sub>4</sub> as the reference. The N<sub>2</sub>-sorption measurements were performed at 77 K using a Micromeritics Tristar 3000 analyzer. Raman spectra were recorded on a microscopic confocal Raman spectrometer (Renishaw 1000 NR) with excitation of 514 nm laser light. Room temperature photoluminescence (PL) was recorded on a Hitachi F-4600 fluorescence spectrophotometer. X-Ray photoelectron spectra (XPS) were performed on an ESCALAB 250 (Thermo Scientific Ltd.), with monochromated aluminium K $\alpha$  X-rays at 1486.6 eV under ultrahigh vacuum conditions.

**Preparation of defect-rich CeO<sub>2</sub> nanorods:** Samples were synthesized by a facile one step hydrothermal process. In a typical hydrothermal procedure, 10 mL aqueous solution of Ce(NO<sub>3</sub>)<sub>3</sub>·6H<sub>2</sub>O (1.5 g) was added to 30 mL deionized water dissolved with 9.6 g NaOH. This mixture was kept stirring for 30 min with the formation of a milky suspension and added into a 50 mL Teflon-lined autoclave with a stainless steel tank. The autoclave was subjected to the hydrothermal treatment at 110 °C for 24 h. Afterwards, the samples obtained were rinsed with deionized water and anhydrous ethanol for several times respectively, then undergo freeze drying and oven drying overnight in air at 60 °C successively. Activity recovery: after prolonged (>20 hours) irradiation, the exhausted nanorods were loaded into NaBH<sub>4</sub> aqueous solution (0.1 M) under stirring. After 1h, the precipitates were collected, purified with distilled water and anhydrous ethanol, and dried in air at 60 °C.

**Photochemical reaction:** The gas-phase CO<sub>2</sub> reduction was operated in a sealed Pyrex cell (600ml, CeO<sub>2</sub> 50 mg), equipped with a quartz window and a double-walled cooling jacket. Prior to the irradiation of a Xe lamp (500 W) the cell was purged with dry nitrogen, followed by the injection of CO<sub>2</sub> (400 ppm). During the whole process the temperature was kept at 25°C, and the headspace gas was regularly monitored by

GC analysis. The GC analysis ( $\text{CO}$ ,  $\text{CO}_2$ ,  $\text{CH}_4$ ,  $\text{O}_2$ ,  $\text{H}_2$ ) was operated on a GC 7900 (Techcomp, Shanghai), equipped with a TDX-01, 80-100 mesh packed column, followed by a  $\text{CO}$ ,  $\text{CO}_2$  conversion furnace and a flame ionization detector (FID), and a molecular sieve 5A packed column followed by a TCD detector, with a limit of detection up to 1ppm.

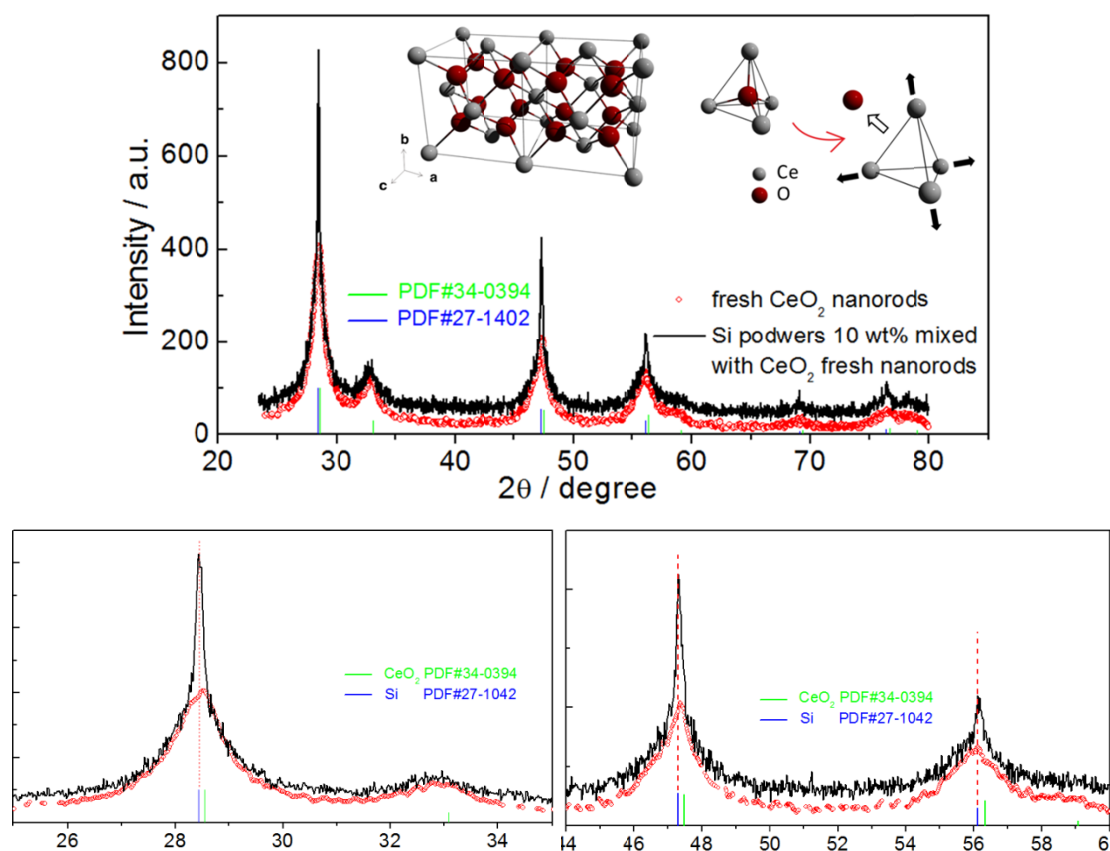


**Figure S1.** X-ray powder diffraction pattern (XRD) of as-prepared  $\text{CeO}_2$  nanorods with inner Si standard. Inset is the tridimensional representation ( $2 \times 1 \times 1$ ) of the cubic fluorite structure. Cerium oxide can be viewed as tetrahedrons with cerium atoms at the corners and oxygen anions at the centers. Cerium oxide with an oxygen vacancy will cause the Ce cations at the corners of one tetrahedron to repel each other because of coulombic interactions, introducing the lattice expansion and local strain.

The broadening diffraction peaks as well as slight shifts toward the lower angles compared to the standard card indicate some sort of lattice expansion and local strain arising from the concomitant O vacancies and  $\text{Ce}^{3+}$  ions.

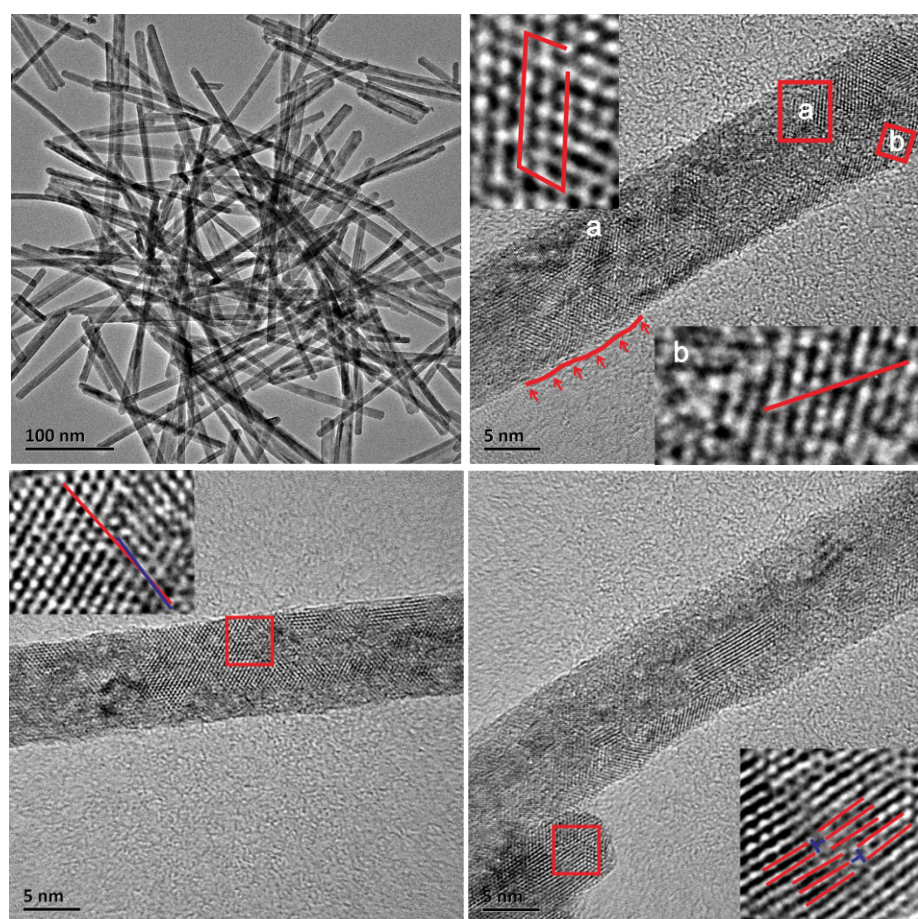


**Figure S2.** HRTEM images of a single nanorod. Defects such like dislocations are surrounded by colored rectangles. Insets are enlarged view of labeled region.

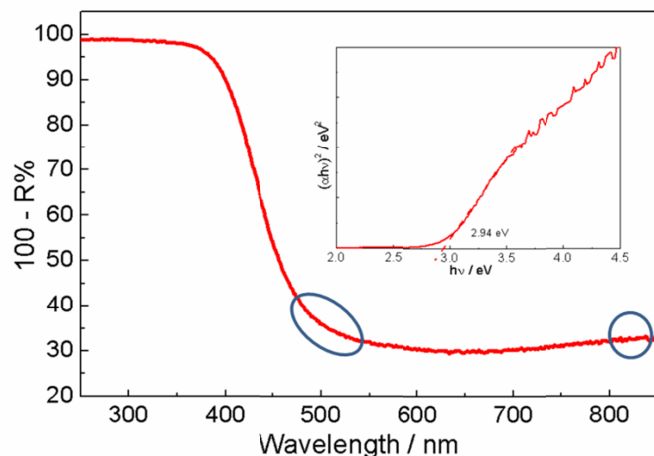


**Figure S3.** UV–vis diffuse reflectance spectra (DRS) of as-prepared CeO<sub>2</sub> nanorods. Inset is the band gap estimation of as-prepared CeO<sub>2</sub> nanorods.

The band gap is estimated to be 2.94 eV approximately, presenting slightly narrowing compared to the reported value for bulk ceria (3.0–3.2 eV). The red shift of absorption onset can be attributed to presence of abundant defects (O vacancies).

The shoulder-like absorption onset extended into the visible region as well as the tail absorption can also be attributable to the defect-related properties.

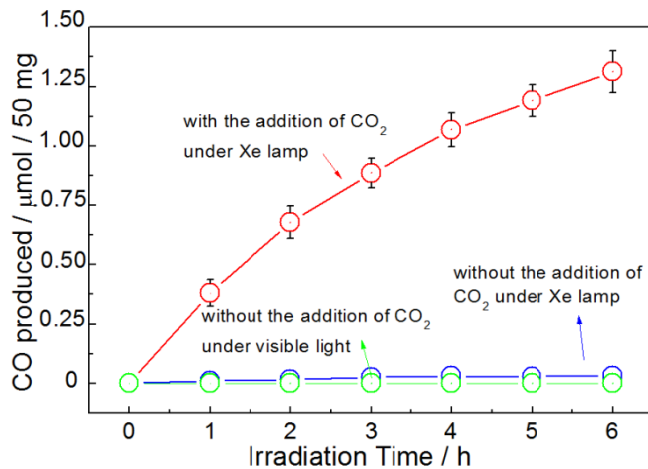


**Figure S4.** CO produced during  $\text{CO}_2$  conversion over fresh  $\text{CeO}_2$  nanorods with or without the addition of  $\text{CO}_2$  into the sealed reactor full of  $\text{N}_2$ .

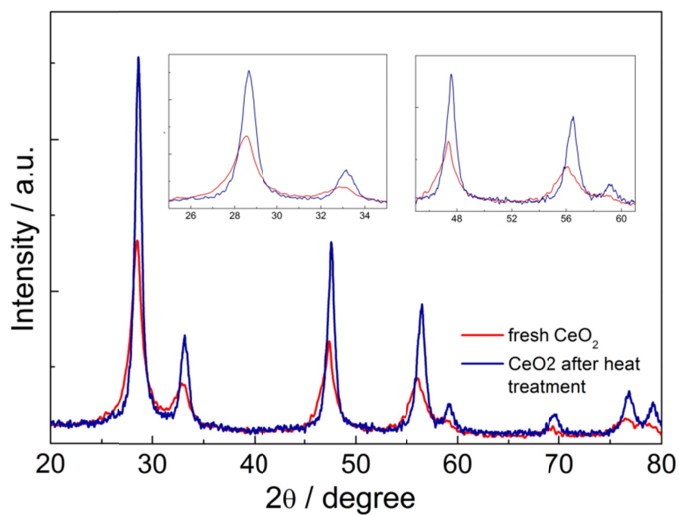


**Figure S5.** X-ray powder diffraction patterns of fresh  $\text{CeO}_2$  nanorods and samples after the heat treatment in  $\text{N}_2$ . Insets are enlarged view for the comparison.

The diffraction peaks of  $\text{CeO}_2$  nanorods after the heat treatment present a narrower and stronger form, as well as slight shift toward higher angles probably indicating the imperfect crystallinity being improved with the elimination of local strain.

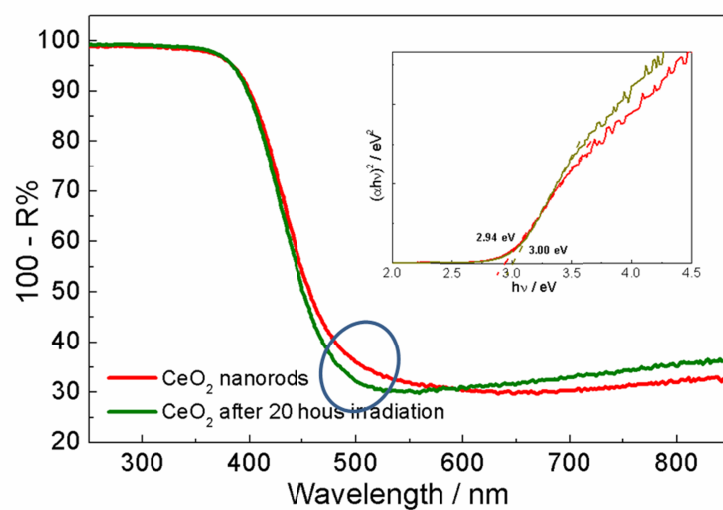


**Figure S6.** UV–vis diffuse reflectance spectra (DRS) of as-prepared  $\text{CeO}_2$  nanorods and samples after 20 hours irradiation. Inset is the band gap estimation.

After 20 hours irradiation, the DRS of exhausted ceria nanorods presented slight reduction around the absorption edge in the visible light region. This variation of DRS might be attributed to the elimination of part of surface defects such like oxygen vacancies.

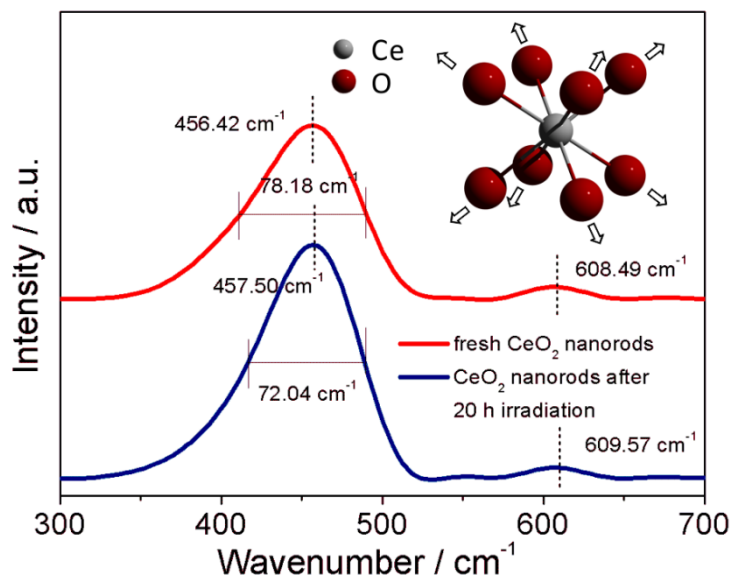


**Figure S7.** Raman spectra of fresh CeO<sub>2</sub> and samples after 20 hours irradiation. Inset is the tridimensional representation of the active F 2g Raman mode. It can be viewed as a symmetrical stretching vibration of the oxygen atoms around cerium ions, sensitive to the local strain.

The Raman spectra of the CeO<sub>2</sub> samples are dominated by the strong F2g mode at about 460 cm<sup>-1</sup>, with a weak peak at about 610 cm<sup>-1</sup> due to a Frenkel-type oxygen defect-induced mode. For fresh samples a much broader F2g peak at ca. 460 cm<sup>-1</sup> indicates greater inhomogeneous strain within the nanorods. We could infer that the surface O vacancies in CeO<sub>2</sub> nanorods were partially eliminated during exhaustive photoreaction with CO<sub>2</sub> from that, after 20 hours photoirradiation the area proportion of 610 cm<sup>-1</sup> peak attributable to O vacancies decreased.

**Table S1.** Curve-Fitting Results from Ce 3d XPS Data

entry	Ce 3d binding energies (eV) and relative amounts (%)* for two subpeaks of Ce <sup>3+</sup>			Ce <sup>3+</sup> / (Ce <sup>3+</sup> +Ce <sup>4+</sup> ) (%)	
	Ce <sup>3+</sup>		Ce <sup>3+</sup> + Ce <sup>4+</sup>		
	v'	u'			
CeO <sub>2</sub> -fresh	887.99 / 3.96	904.64 / 3.96	1	7.92	
CeO <sub>2</sub> -photo**	887.77 / 3.43	904.82 / 3.86	1	7.29	

\*The relative amounts (%) of Ce<sup>3+</sup> were calculated from the areas under the curves for each subpeak.

\*\*CeO<sub>2</sub>-photo represents the exhausted CeO<sub>2</sub> nanorods after 20 hours photoirradiation.

**Table S2.** Curve-Fitting Results from O 1s XPS Data

entry	O 1s binding energies (eV) and relative amount of oxygen species (%)*				(O <sub>2</sub> <sup>2-</sup> +O <sub>2</sub> <sup>-</sup> ) / O <sup>2-</sup>
	O <sup>2-</sup>	O <sub>2</sub> <sup>2-</sup>	CO <sub>3</sub> <sup>2-</sup> / OH <sup>-</sup>	O <sub>2</sub> <sup>-</sup>	
CeO <sub>2</sub> -fresh	529.72	531.38	532.60	-	0.68
	45.18	30.56	24.26	-	
CeO <sub>2</sub> -photo**	529.81	531.32	532.45	533.67	1.28
	36.18	30.42	17.64	15.77	

\* The relative amounts (%) of various oxygen species were calculated from the areas under the curves for each subpeak.

\*\*CeO<sub>2</sub>-photo represents the exhausted CeO<sub>2</sub> nanorods after 20 hours irradiation.